Earliest Miocene calcareous nannofossil biostratigraphy from the low-latitude Pisco Basin (Peru)

Emilia R Belia[1], Kevin E Nick[1], Erika Bedoya Agudelo[2] and David K Watkins[3]
[1]*Department of Earth and Biological Sciences, Loma Linda University, Griggs Hall, Room 101, Loma Linda, CA 92350-1702, USA*
[2]*CADIC- Centro Austral de Investigaciones Científicas. Bernardo Houssay 200, CP9410 Ushuaia, Tierra del Fuego, Argentina*
[3]*Department of Earth and Atmospheric Sciences, University of Nebraska, Lincoln, NE 68588-0340, USA*
email: emyrut@gmail.com

ABSTRACT: Stratigraphic studies, based on lithology, diatoms, and mollusks, have suggested different chronostratigraphic placements for formations in the Pisco Basin. This study focusses on a stratigraphically important, calcareous nannofossil-bearing unit between the Chilcatay and Pisco formations. The Eocene-Pliocene Pisco Basin is located at low latitude (-14°S) in a forearc basin in central coastal Peru. The objective of this study is to use nannofossil biostratigraphy to constrain the age of an interval for ongoing stratigraphic work in the region. We analyzed nannofossils from two sections located on the northern end of the Cerros Yesera de Amara trend and in Cerro Las Tres Piramides. A tuff bed above the top of the section is dated to 17.70 ±0.24 Ma based on a single Ar-Ar age from biotite. Analysis of productive samples from the two locations show rare to common calcareous nannofossil occurrence with poor to moderate preservation. Nannofossils show strong dissolution and/or overgrowth in almost all samples. Based on the first occurrence (FO) of *Helicosphaera carteri* in association with *Cyclicargolithus abisectus*, *Reticulofenestra bisecta*, and *Triquetrorhabdulus carinatus*, we suggest that the assemblage recovered represents an age of earliest Miocene, Zone NN1 (CN1b). Studies from the equatorial Pacific region indicate rare and discontinuous occurrence of *Reticulofenestra bisecta* (<10 µm) in late Oligocene and earliest Miocene (NN1), making it difficult to determine if its occurrence in the assemblage is caused either by low productivity or by reworking. The absence of *Discoaster druggii* might suggest that the assemblage is not younger than NN1, although *Discoaster druggii* tends to be rare and difficult to find even in well preserved sediments.

INTRODUCTION

The Pisco Basin is located along the coast of Peru (text-figure 1A) and contains a sedimentary record reflecting tectonic and marine conditions through the significant events of the Cenozoic. Fossiliferous sediments were deposited in the Pisco Basin during several transgressive events throughout the Cenozoic (Dunbar et al. 1990). Regional syntheses based on foraminifera (Kennett et al. 1985) and siliceous microfossils (Kamikuri and Moore 2017) suggest significant changes in oceanic circulation patterns for the Pacific in the early Neogene. These changes are recorded at the eastern Pacific margin in the Pisco Basin and may be reflected in cold water microfossil abundance in the upper Miocene (Fourtanier and Macharé 1988; Dunbar et al. 1990).

Relatively few reports of calcareous nannofossils in the Pisco Basin exist in the literature. These reports have documented the occurrence of late Eocene and/or Oligocene (Marty et al. 1988; Dunbar et al. 1990; DeVries et al. 2006) and early Miocene (Dunbar et al. 1990; Di Celma et al. 2018) calcareous nannofossils. Unfortunately, most of these studies did not include species names (Marty et al. 1988) or biozones (DeVries et al. 2006), or are based on personal communication with different authors (Dunbar et al. 1990). None of these references provide complete data on abundance, preservation, and assemblage analysis of the nannofossils recovered. This study improves on previous reports of calcareous nannofossils (Belia et al. 2015; Belia and Nick 2016; Di Celma et al. 2018) in the Pisco Basin.

This study constrains the biostratigraphic age of a calcareous nannofossil-bearing unit close to the boundary between the Chilcatay and Pisco Formations in the Ica River Valley. Stratigraphic studies, based on lithology, diatoms, and mollusks, have suggested different chronostratigraphic placements for formations in the Pisco Basin, particularly for the base of the Pisco (Miocene) and top of the Chilcatay (referenced as Miocene or Oligocene) formations (León et al. 2008; Di Celma et al. 2018; DeVries and Jud 2018).

In addition, this study contributes to development of assemblages for the earliest-Miocene interval from low latitudes of the eastern equatorial Pacific region. Species used to define biozones in the North Sea and North Atlantic may not all be useful at low latitudes. Most biostratigraphic studies based on Cenozoic nannofossils have concentrated in the North Sea (e.g. Perch-Nielsen 1979; Siesser et al. 1987; Varol 1989) and Mediterranean regions (e.g. de Kaenel and Villa 1996; Fornaciari and Rio 1996; Maiorano and Monechi 2006; Kallanxhi et al. 2016). Some species from higher latitudes are difficult to correlate worldwide due to provincialism in floral events (Wei and Wise 1990; Wei et al. 1992). Recent studies (e.g. Raffi et al. 2006; Backman et al. 2012; Agnini et al. 2014) are generating more data from low latitude regions; however, data from the eastern equatorial Pacific are still limited for the earliest Miocene biozones. Many ocean drilling program cruises have drilled in the region, but several did not recover any sediments from the Miocene (e.g. Legs 111, 135, 138, 141, 205, 206) or have reported only scarce data from lowermost

Miocene (e.g. Legs 9, 16, 85, 112, 143, 181, 202) therefore most of the biostratigraphic results from the region are limited to middle Miocene to Pleistocene.

GEOLOGICAL SETTING

A series of forearc basins record the depositional history of the eastern equatorial Pacific from northern Chile to southern Colombia (Suess et al. 1988; Dunbar et al. 1990; Lopez Ramos 2009). Within that trend, the greater Pisco Basin contains one of the best exposed records of the Eocene to lower Pliocene (Klein et al. 2011). The exposed part in the East Pisco Basin is one of three shelf basins bounded by two linear structural trends along the continental margin of Peru (Thornburg and Kulm 1981). The Outer Shelf High was an important topographic feature that created at least a local barrier between the Pisco Basin and the open ocean during the Cenozoic. Basement topography and paleo-highs produced protected and/or semi-protected marine environments in the basin during the Miocene (DeVries 1988; Dunbar et al. 1990). Subsequent uplift and exposure occurred during late Pliocene/Pleistocene (Dunbar et al. 1990).

Sedimentary rocks in the Pisco Basin have been divided into five formations: Caballas, Paracas or Paracas Group (with the Los Choros and Yumaque Formations), Otuma, Chilcatay, and Pisco. In general, there is some controversy on the stratigraphic placement of formation boundaries which are likely time transgressive. Exact placement of formation boundaries is difficult to describe and address in the field because of the similarity of lithology, lack of detailed mapping, and structural complexities. For instance, Dunbar et al. (1990), DeVries (1998), León et al. (2008), and Di Celma et al. (2018) differ in the chronostratigraphic position for the Pisco-Chilcatay contact. Dunbar et al. (1990) and DeVries (1998) established this contact around the middle Miocene and set a hiatus between formations, placing the Chilcatay Formation almost completely in the lower Miocene. Di Celma et al. (2018) also placed the Chilcatay Formation in the lower Miocene. On the other hand, León et al. (2008) placed the contact at the Miocene-Oligocene boundary, with no hiatus, and report the Chilcatay Formation as upper Oligocene.

This study examines a unit located close to the controversial Pisco-Chilcatay boundary. We follow Di Celma et al. (2018) and consider this unit as close to the upper part of the Chilcatay Formation. The studied unit is exposed in the region containing Cerro Yesera de Amara and Cerro Las Tres Piramides, in the Ica River Valley (text-figure 1B). Immediately below the study unit is a distinctive, well-cemented, fossiliferous, siliciclastic unit formed of prograding clinoforms. Below the clinoforms are siltstones, sandstones, and tuffs comprising the Chilcatay Formation. Above the studied unit are diverse lithologies including siltstones, sandstones, tuffs, and diatomaceous siltstones comprising the base of the Pisco Formation.

MATERIALS AND METHODS

The material for the present study was collected from two sections: one at the north end of the Cerro Yesera de Amara trend (section A; -14.5822º S, -75.6823º W) and the second at Cerro Las Tres Piramides (section B; -14.5902º S, -75.6421º W) (text-figures 1 and 2). We used two lithostratigraphic markers to help identify and correlate the sections across the study area within the Ica River drainage. All sections are above and within sight of exposures of the shelly and coarse-grained clinoform beds of the Chilcatay. The base of the sections is marked by a distinct orange-red weathering dolomite that crops out just above the clinoform beds and a phosphatic-pebble rich layer with andesite pebbles and cobbles marks the top of the sections. The dolomite bed was mapped across the studied area as a datum for correlation (text-figures 1B and 2).

Section thickness was determined by a combination of differential GPS and laser range finder measurements corrected for dip. Strata typically dip at low angles of less than 4° in the area of study, though outcrops are separated in many cases by faults. We described sections A and B and collected a total of 30 samples of fine-grained clastic rocks that showed reaction to acid or had visible foraminifera in the field. Samples were stored in puncture resistant bags to avoid contamination. The number of, and spacing between, samples was based on the thickness of each depositional layer evaluated in the field by grain size and color, resulting in a sample approximately every 10-45 cm.

In the lab, samples were prepared by smear slide technique (Perch-Nielsen 1985; Bown and Young 1998). Each slide was observed using a BX51-P polarizing microscope and full-wave (gypsum) accessory plate at 1000X. In addition, we processed 3 samples (B14-3B-14, B14-3B-15, and B15-3B16) for scanning electron microscope (SEM, TESCAN VEGA II) observations (Bown and Young 1998). All sample preparation and microscopy took place in the Department of Earth and Biological Sciences, Loma Linda University (LLU).

Samples were analyzed for grain size using a Beckman Coulter LS 13 320 laser diffraction particle size instrument. We disaggregated the samples in a $NaCO_3$ buffer with sonication for about 10 seconds, then circulated the slurry through the particle analyzer with sonication. Grain size cutoffs in the software were used to estimate the percent of clay, silt and sand in the samples. Grain size analysis was done at the Department of Earth and Biological Sciences, LLU.

Identification to species level is based on the taxonomy references from Perch-Nielsen (1985) and Young (1998) and complemented by catalogues from the Nannotax3 (http://www.mikrotax.org/Nannotax3/). We followed the standard zonation of Martini (1971) and Okada and Bukry (1980). We also compared our results with the zonal scheme proposed by Backman et al. (2012) and Agnini et al. (2014) since some markers proposed by Martini (1971) and Okada and Bukry (1980) are absent.

Relative abundance was estimated by a semi-quantitative method (Roth and Thierstein 1972) as follow: Abundant (A) = more than 10 specimens per FOV (field of view); Common (C) = 10 to 1 specimens per FOV; Few (F) = 1 specimen per one to ten FOVs; Rare (R) = 1 specimen per more than ten FOVs, Questionable (?) = questionable presence of this species, and Barren (B) = none observed. We counted each slide in three full traverses (~360 fields of view) per slide and in samples with low abundance or poor preservation; additional traverses were scanned for rare species. Preservation of nannofossils was evaluated qualitatively based on observation of dissolution and overgrowth as follows: Good (G) = individual specimens exhibit little or no dissolution and/or overgrowth, Moderate (M) = individual specimens exhibit little or some dissolution and/or overgrowth, but are still identifiable, Poor (P) = individual specimens exhibit serious effects of dissolution and/or overgrowth of diagnostic elements.

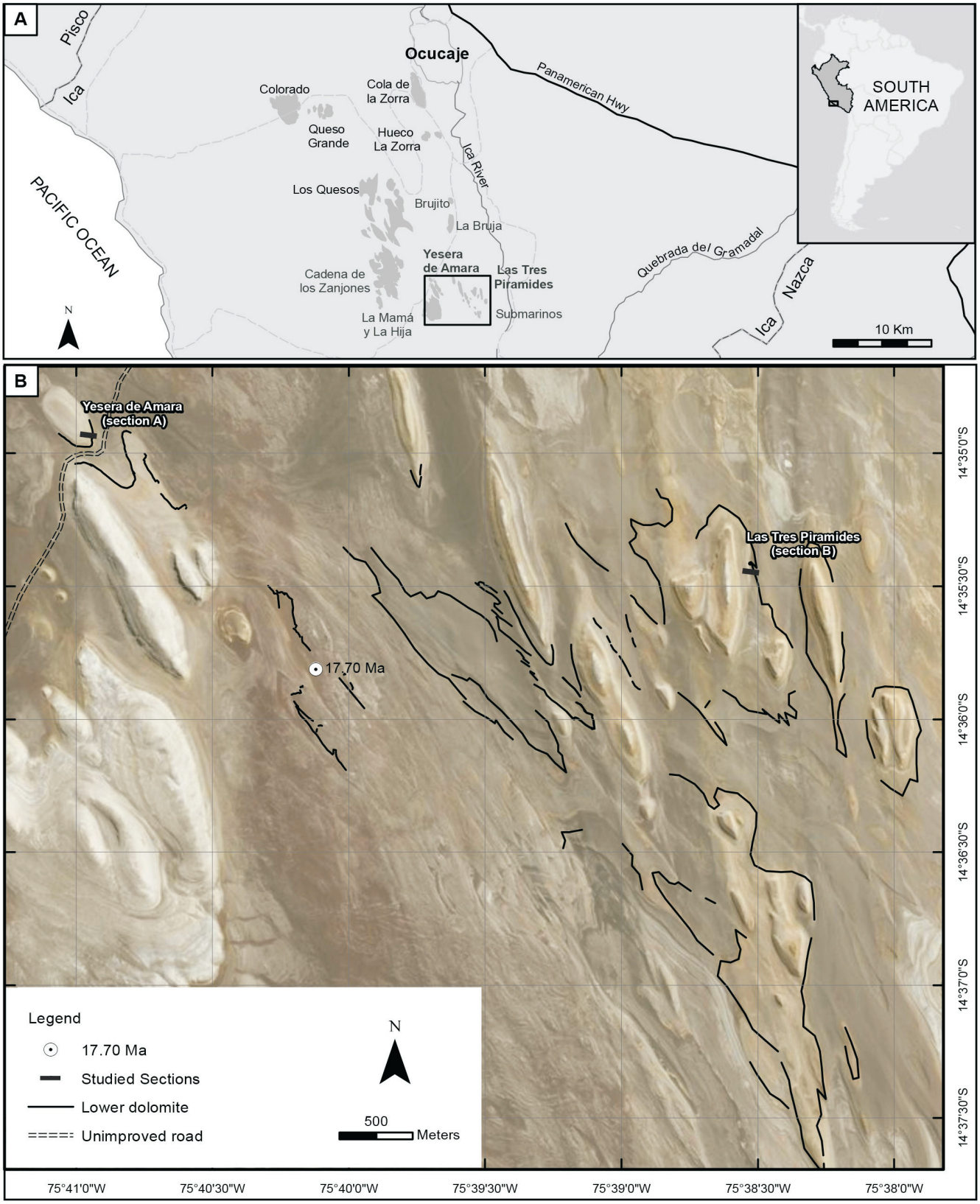

TEXT-FIGURE 1
Location of study area in Peru. (A) Study area (square) in relation to the town of Ocucaje and hills. (B) Location of studied sections. Thin black lines represent dolomite cemented beds near the base of the sections. White circle shows the sample location for the Ar-Ar biotite age from a tuff bed. The 17.70 Ma date is stratigraphically above the measured sections.

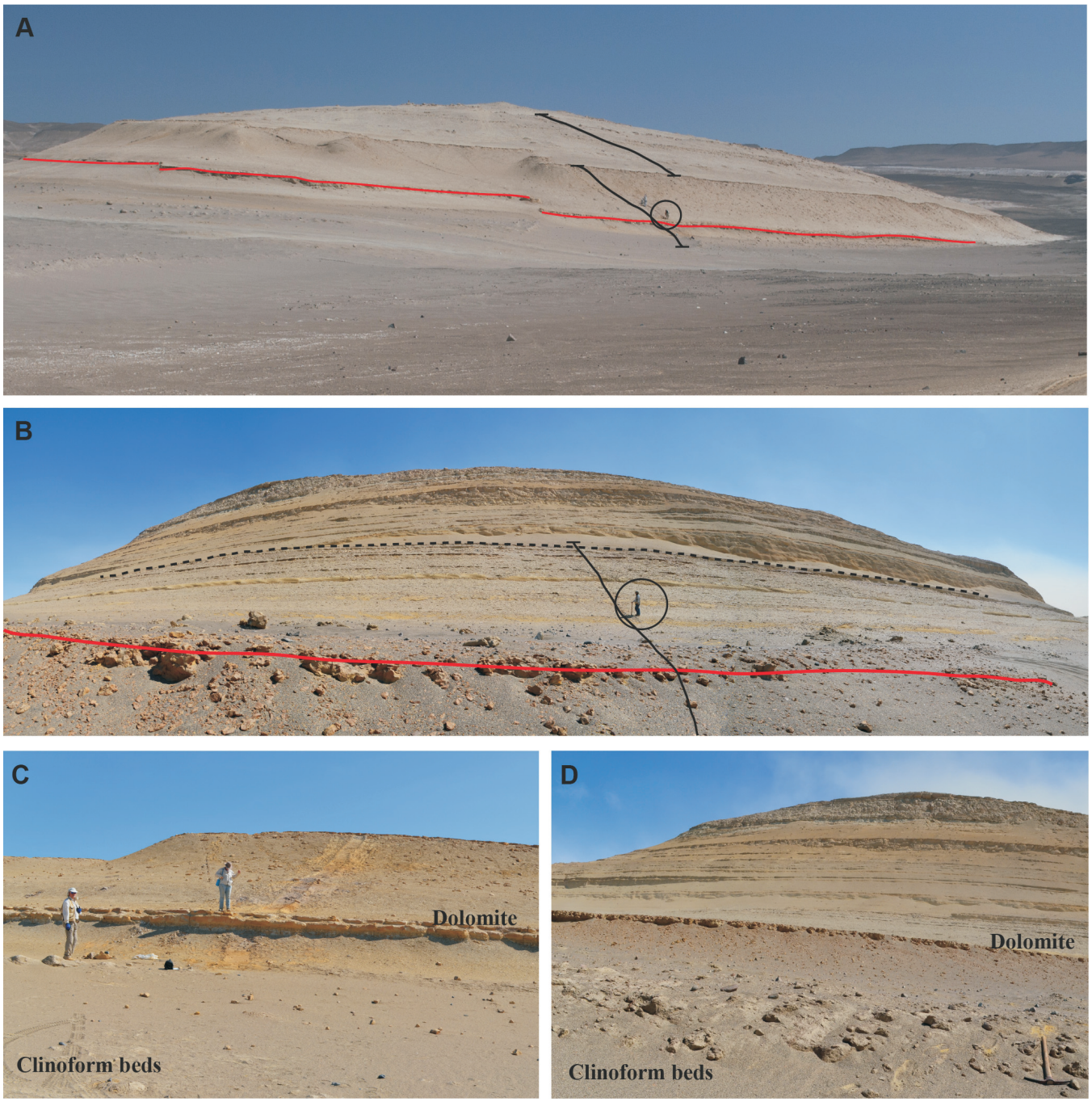

TEXT-FIGURE 2
Outcrop photographs. (A) Southeast facing slope of the hill at the north end of Cerro Yesera de Amara, section A (circle indicates person for scale) and (B) east facing slope at Cerro Las Tres Piramides, section B (circle indicates person for scale). Black lines on outcrops show locations of sections with red lines marking the lower dolomite and dashed line marking the phosphatic bed. (C) The orange-red dolomite at the base of the section in Yesera de Amara and (D) Las Tres Piramides. Clinoform beds dip in sets below the dolomite bed.

In addition, four other outcrops were located and correlated using the two lithostratigraphic markers (orange-red dolomite and a phosphatic-pebble rich layer) across the study area. We used the data from these locations to verify the occurrence of nannofossils between our two lithostratigraphic markers. Coordinate locations of the sections are in Appendix 1.

We also processed all samples productive for calcareous nannofossils (22) collected from Cerro Yesera de Amara to extract foraminifera. Each sample was disaggregated by simple soaking in water buffered with sodium carbonate. After approximately 24 hours soaking, samples were wet screened through a 50 μm sieve and the coarse fraction dried. Foraminifera were picked under a stereomicroscope and transferred to gela-

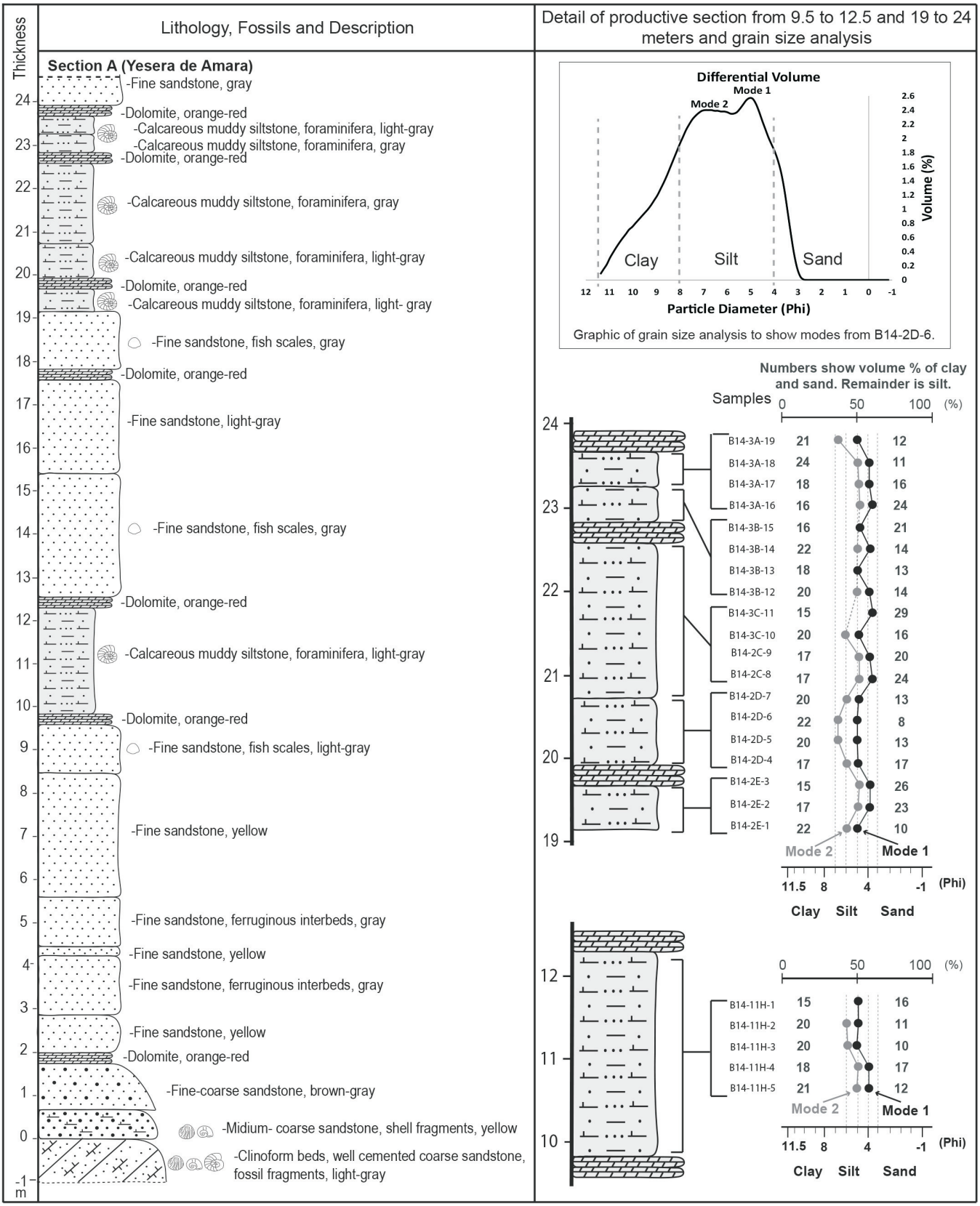

TEXT-FIGURE 3
Measured section with lithologies and locations of analyzed samples from Cerro Yesera de Amara (section A). Productive samples are calcareous muddy siltstone and all also contain foraminifera. Grain size analysis shows little variation among samples. Dolomites were not productive.

tin-coated SEM stubs and imaged. Kenneth Finger from the Museum of Paleontology, University of California, Berkeley assisted with analysis of the SEM images.

RESULTS

Stratigraphic sections

The stratigraphic sections are bounded at the base by one to three thick and closely-spaced beds of distinct orange-red weathering dolomite (**text-figure 1B**) and at the top by a phosphatic-pebble rich layer with andesite pebbles and cobbles. These lithostratigraphic markers can be traced over an area of approximately 13 km^2 between the stratigraphic sections.

Biotite crystals were extracted from near the base of a 7 cm thick tuff at 14.59832°S, 75.66959°W for dating. They yielded an Ar-Ar date of 17.70±0.24 Ma based on 7 heating steps, 63.2% Ar released, and an MSWD of 0.04. This tuff bed is stratigraphically above the sampled sections, but is about 2 km from either section. Because of low relief and distance, we were not able to measure an exact stratigraphic thickness from the top of either section to the tuff bed, but estimate the thickness to be between 5 and 20 m.

Modal grain sizes are shown for twenty-four samples from the middle and upper part of section A in text-figure 3 and for six samples from the middle part of the section B in text-figure 4. In both sections, laser scattering algorithms give two closely spaced grain size modes in almost all samples: Mode 1 (black circles) is coarser and Mode 2 (gray circles) is finer by about 1.5 phi. An example of two differential volumes from one sample (B14-2D-6) is shown in text-figure 3. The modes are shown next to each sample references with the volume % (Phi) of clay, sand, and the remain is silt. Based on these results, we categorized the samples collected from section A as calcareous muddy siltstone, and section B as calcareous sandy siltstone.

Section A (text-figures 3) is 25 m thick and is composed mainly of fine sandstone, calcareous muddy siltstone containing foraminifera and orange-red dolomite beds. Sandstones vary in a range of colors from light-gray to brown-gray, and yellow. The clinoform beds dip in sets below the lower dolomite bed and are extended longshore for hundreds of meters to kilometers (text-figure 2 A and **C**). The clinoform beds are a well cemented coarse sandstone with fossil fragments (shells, gastropods, etc.).

Section B (text-figures 4) is located 4.42 km east of section A and is 19 m thick between the dolomite-rich (bottom) and phosphate pebble-rich (top) marker beds, which were used to correlate the sections. Section B is composed mainly of silty to fine sandstone, calcareous sandy siltstone, and orange-red dolomite beds. Sandstones vary in a range of colors from light-gray to gray, and yellow. As in section A, the clinoform beds are found below the lower dolomite (text-figure 2 B and D).

Calcareous nannofossil assemblage richness and preservation

The distribution of the identified nannofossil taxa is shown in **text-figure 5**. Section A and B are shown in different tables to be clear to the reader. Although analysis of both sections showed some differences between the assemblages (e.g. abundance and preservation), the occurrence of key species in both assemblages suggest the same age. Representative nannofossil taxa are illustrated in Plates 1 and 2. An alphabetic list of calcareous nannofossil cited in the text and figures is included in Appendix 2.

The nannofossil species abundance in section A is rare to common in the twenty-two productive samples. The species richness is moderate, comprising a total of 33 nannofossil taxa. The assemblage consists of the genera *Calcidiscus*, *Coccolithus*, *Coronocyclus*, *Cyclicargolithus*, *Discoaster*, *Helicosphaera*, *Pontosphaera*, *Reticulofenestra*, *Sphenolithus,* and *Triquetrorhabdulus*. In general, preservation is poor to moderate, showing strong dissolution and/or overgrowth in almost all samples. Most of the larger coccoliths (e.g. *Coccolithus pelagicus*) show overgrowth on the distal shield elements (text-figure 6, A). In general, discoasters are too poorly preserved to identify to the species level. For instance, they are overgrown around the central area and along rays (text-figure 6, B, Plate 2 Fig. 13 and 14). *Helicosphaera* and *Reticulofenestra* exhibit dissolution and/or overgrowth on the central area and shields (text-figure 6, C and D). Regardless of the general preservation, the occurrence of coccospheres (e.g. coccospheres of *Reticulofenestra* and *Cyclicargolithus floridanus* text-figure 6, E and F; Plate 2, Fig. 27-30) in most of the samples suggests minimal bioturbation/transport.

In section B (text-figure 5) nannofossil occurrence is rare to common in the four productive samples. However, the overall abundance is considerably decreased (< 8 specimens occur in one field of view) and preservation is worse than in samples from section A, hampering species level identification. Species richness is moderate, comprising a total of 27 nannofossil taxa. The assemblage consists of the genera *Calcidiscus*, *Coccolithus*, *Cyclicargolithus*, *Discoaster*, *Helicosphaera*, *Reticulofenestra*, *Sphenolithus,* and *Triquetrorhabdulus*. The difference in abundance and preservation of nannofossils in both sections might be related to the coarser grain size in section B.

Other microfossils found in the samples

Samples collected from sections A and B contain benthic and planktonic foraminifera and two samples from section A-2 (additional section, Appendix 1) contain diatoms. The foraminifera are poorly preserved and diagnostic features for species determination are not evident by light or electron microscopy (Kenneth Finger, personal communication, April 16, 2018). Genera identified did not help constrain the biostratigraphic age of the unit. The diatoms observed in the sample B14-22A and B14-22A-1 are mostly broken and only *Thalassionema nitzschioides* (Grunow) Van Heurck 1896 was identified (Angelo Plata, personal communication, December 26, 2018). This species has a wide age range, from early Oligocene (31.2 Ma) to the Recent.

INTERPRETATION AND DISCUSSION

Calcareous nannofossil assemblage

Dolomitic and phosphatic beds marking the base and top of the sections can be mapped over a large area and therefore we are confident basing our assemblage on combined results from both sections. Combined data indicate an assemblage comprised by *Coccolithus pelagicus*, *Cyclicargolithus abisectus* (> 11 μm), *Cyclicargolithus floridanus*, *Discoaster deflandrei*, *Helicosphaera carteri*, *Reticulofenestra* (3-5 μm and 5-7 μm), *Reticulofenestra dictyoda*, *Reticulofenestra lockeri*, and *Sphenolithus moriformis*. Rare *Calcidiscus pataecus*, *Helicosphaera euphratis*, *Helicosphaera granulata, Helicosphaera obliqua,*

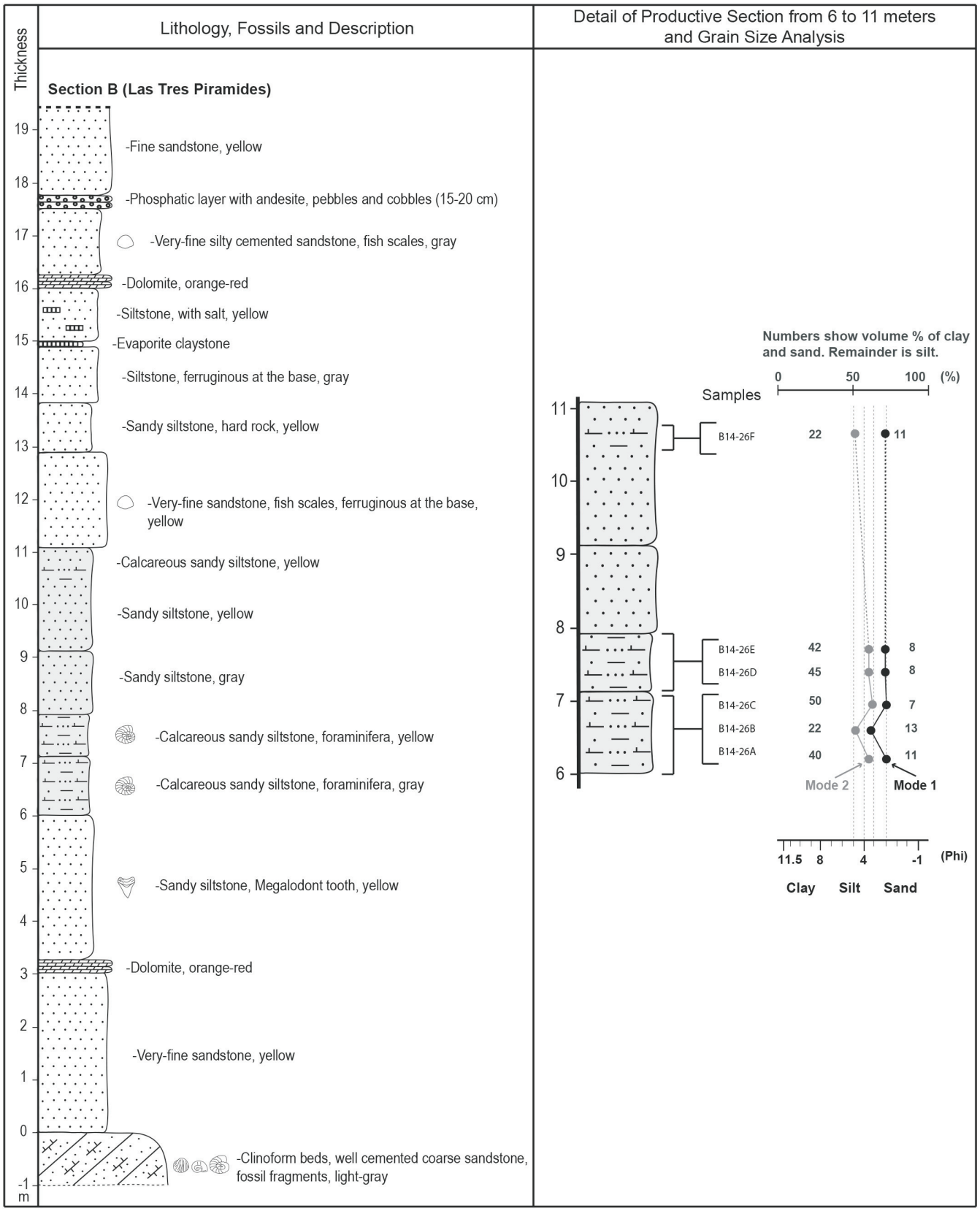

TEXT-FIGURE 4
Measured section with lithologies and locations of analyzed samples from Cerro Las Tres Piramides (section B). Productive samples are calcareous sandy siltstone and all also contain foraminifera. Grain size analysis shows little variation among samples. Dolomites were not productive.

Reticulofenestra bisecta (<10 μm), *Reticulofenestra minuta, Sphenolithus conicus*, *Sphenolithus dissimilis*, and *Triquetrorhabdulus carinatus* were also observed. Reworked species (*Chiasmolithus* sp.) are rare in the assemblage and found only in section A (text-figure 5).

Calcareous nannofossil biostratigraphy

We based our biozone assignments (**text-figure 7**) mostly on the works of Martini (1971) and Okada and Bukry (1980). The zonal schemes proposed for the Paleogene by Agnini et al. (2014) and Neogene by Backman et al. (2012) are included in text-figure 7, but their schemes use *Sphenolithus* and *Discoaster* species which are not preserved well enough in our samples to identify to species level. First, we define the latest Oligocene Zones NP25 (or Subzones CP19b and CN1a) and earliest Miocene Zone NN1 (or Subzone CN1b). Then, we describe the occurrence of *Reticulofenestra bisecta*, *Helicosphaera carteri*, *Cyclicargolithus abisectus*, and *Triquetrorhabdulus carinatus* in the assemblage. Finally, we discuss about the occurrence and/or absence of some sphenoliths in the samples. The species mentioned in the discussion are included in text-figure 7.

In addition, we compare our results with publications from the eastern equatorial Pacific region. Seven Sites from selected Legs (recovered uppermost Oligocene and/or lower Miocene calcareous nannofossils) are included for the discussion. Sites 682 and 688 (ODP Leg 112) were cored in the forearc basin and continental slope of the convergent margin off Peru (Martini 1990) and are close to the Pisco Basin. Site 1218 (ODP Leg 199) was recovered in the central part of the tropical Pacific Ocean (Blaj et al. 2009; Backman et al. 2012; Agnini et al. 2014). Sites U1331- U1334 (IODP Expedition 320) were drilled in the central Pacific, to the southeast of ODP Site 1218 (Pälike et al. 2010; Bown and Dunkley Jones 2012). Onshore, our search of the literature found two publications (Mejía et al. 2007; Mejía-Molina et al. 2010) from northern Colombia and three publication from Pisco Basin (Belia et al. 2015; Belia and Nick 2016; Di Celma et al. 2018) reporting earliest-Miocene nannofossils.

Definition of the biozones around the Oligocene/Miocene boundary

Sphenolithus ciperoensis Zone (NP25 or Subzones CP19b and CN1a): Martini (1971) defined the *Sphenolithus ciperoensis* Zone (NP25) as the interval from the last occurrence (LO) of *Sphenolithus distentus* to the LO of *Helicosphaera recta* (text-figure 7). The lower and middle part of Zone NP25 is correlated to the *Dictyococcites bisectus* Subzone (CP19b) of Okada and Bukry (1980). The top of CP19b is based on the LO of *Sphenolithus ciperoensis* and is commonly used for the top of Zone NP25. Bukry (1973) also included the LO *Dictyococcites bisectus* (=*Reticulofenestra bisecta*) as an auxiliary marker for the top of Subzone CP19b. Zone CNO5 of Agnini et al. (2014) correspond to the CP19b Subzone, and is the interval defined from the top of *Sphenolithus predistentus* to the top of *Sphenolithus ciperoensis*.

The upper part of Zone NP25 (Martini, 1971) corresponds to the Subzone CN1a and lowermost Subzone CN1b of Okada and Bukry (1980). Okada and Bukry defined the Subzone CN1a by the LO of *Sphenolithus ciperoensis* and *Dictyococcites bisectus* (=*Reticulofenestra bisecta*) to the end of the "acme" of *Cyclicargolithus abisectus*. The Subzone CN1a and lowermost Subzone CN1b correspond to the Partial Range Zone (CNO6) of Agnini et al. (2014) defined by the interval from Top *Sphenolithus ciperoensis* to Top *Sphenolithus delphix*.

Triquetrorhabdulus carinatus Zone (NN1 or Subzone CN1b): Martini (1971) defined the *Triquetrorhabdulus carinatus* Zone (NN1) by the disappearance of *Helicosphaera recta* to the appearance of *Discoaster druggi*. Zone NN1 correlates to CN1b of Okada and Bukry (1980) and approximately to Zone CNM1 of Backman et al. (2012) which is defined as the interval between the top of *Sphenolithus delphix* and base of *Sphenolithus disbelemnos*.

In general, it is accepted that the Oligocene-Miocene boundary is placed at the Chattian-Aquitanian boundary, as stated in Gradstein et al. (2012). Martini (1971) placed this boundary within the base of nannofossil Zone NN1 (Neogene). Okada and Bukry (1980) defined this boundary as CP19b/CN1 (Paleogene/Neogene), but later it was placed at the top of CN1a.

Occurrence of Reticulofenestra bisecta

Two similar forms, *Reticulofenestra bisecta* (5-10 μm) and *Reticulofenestra stavensis* (> 10 μm) are distinguished by size. All the *Reticulofenestra* observed in our samples are 5 to10 μm, with none larger than 10 μm. Two examples are shown in Plate 1, Fig. 14-15 (10 μm) and Plate 1, Fig. 16-17 (7 μm). The occurrence of *Reticulofenestra bisecta* in our samples suggests that the assemblage might represent an age close to the Oligocene/Miocene (CN1a/CN1b) boundary. Okada and Bukry (1980) defined this boundary by the LO of *Dictyococcytes bisecta* (=*Reticulofenestra bisecta*). *Reticulofenestra stavensis* goes extinct before the Oligocene-Miocene boundary. Our samples do not contain these large forms, suggesting an early Miocene age for our assemblage.

As noted from studies located in the equatorial Pacific region, the occurrence of *Reticulofenestra bisecta* (< 10 μm) becomes rare and discontinuous in the late Oligocene. For instance, Martini (1990) documented *Reticulofenestra bisecta* (referenced as *Dictyococcites dictyodus*) as rare and discontinuous in the late Oligocene, combined Zone NP24/25 (Table 5, p. 223) at Site 682 (Leg 112). Bown and Dunkley Jones (2012) also reported the sporadic occurrence of *Reticulofenestra bisecta* (<10 μm, Chart 4, p. 22) in late Oligocene at Site U1334 (Expedition 320). They also observed that *Reticulofenestra bisecta* (< 10 μm) barely gets into the NN1 at the same Site (Chart 4, p. 22). Confusion on the use of *Reticulofenestra* for biozone interpretation is complicated since many publications have not recorded the coccolith size. Our species are small and their abundance is low.

Some authors used the LOs of *Reticulofenestra bisecta* together with *Zygrhablithus bijugatus* to define late Oligocene biozones. For instance, Martini (1990) used the LOs of "*Dictyococcites dictyodus"* (=*Reticulofenestra bisecta*) and *Zygrhablithus bijugatus* to define the top of a combined Biozone NP24/25 at Site 682 (Leg 112). Nevertheless, Mejía-Molina (2010) identified the LO of *Zygrhablithus bijugatus* before the LO of *Reticulofenestra bisecta* at Arroyo Alférez and Estratigráfico 4 (Colombia). The absence of *Zygrhablithus bijugatus* in our assemblage also might suggest an early Miocene age.

AGE	SECTION	SAMPLES (B14-)	ABUNDANCE	PRESERVATION	*Calcidiscus pataecus*	*Calcidiscus* sp. (< 5 µm)	*Coccolithus miopelagicus*	*Coccolithus pelagicus*	*Coccosphere indet.*	*Coronocyclus nitescens*	*Cyclicargolithus abisectus* (>11 µm)	*Cyclicargolithus floridanus*	*Discoaster deflandrei*	*Discoaster* sp.	*Helicosphaera carteri*	*Helicosphaera euphratis*	*Helicosphaera granulata*	*Helicosphaera obliqua*	*Helicosphaera* sp.	*Helicosphaera* sp. *cf. H. recta*	*Pontosphaera multipora*	*Pontosphaera* sp.	*Pyrocyclus* sp.	*Reticulofenestra bisecta* (< 10 µm)	*Reticulofenestra daviesii*	*Reticulofenestra dictyoda*	*Reticulofenestra lockeri*	*Reticulofenestra minuta*	*Reticulofenestra* sp. (3-5 µm)	*Reticulofenestra* sp. (5-7 µm)	*Sphenolithus conicus*	*Sphenolithus dissimilis*	*Sphenolithus moriformis*	*Sphenolithus* sp.	*Thoracosphaera heimii*	*Thoracosphaera* sp.	*Thriquetrorhabdulus carinatus*	*Chiasmolithus* sp. (Reworked)
EARLIEST MIOCENE	SECTION A	3A-19	A	M				F	R	R	R	F	F	R	F		R	R	R							R	R	R	R	R		R		R		R
		3A-18	A	M				F	R	R	R	F	R	R	R	R	?		R				R			R	R		R		R			R			R
		3A-17	A	M	R			F	R	R	R	F	F	R	R	R			R		R	R	?	R		R	R		R		R	R	R			R		R
		3A-16	A	M			R	F	R		R	F	R	R	R				R				R	R		R	R		R		R	R	R	R				
		3B-15	C	M		R	R	F	R	R		F	R	R	R	R	R		R				R	R	R	R	R	R		R	R	R		R				
		3B-14	A	M	R			C	R	R	R	F	R	R	R	?	R	R	R		R	R	R	R		R	R		R	R	R	?	?	R				
		3B-13	C	P/M	R	R		C	R	R	R	F	R	R	R	R	R		R	R			R	R		R	R		R	R	R	R	R	R	R		R	
		3B-12	C	P/M				R					R	R	R									R			R				R			R				
		3C-11	C	P/M	R			F	R	R	R	F	R	R	R				R				?	R			R				R			R			R	
		3C-10	C	P/M		R	R	C	R	R	R	F	R	R	R				R				R	R		R	R				R	?	R	R	R			
		2C-9	F	P/M				R				R	R	R																		R						
		2C-8	B																																			
		2D-7	F	P/M		R	R	R			R	R	R	R										R		R	R				R	R	R	R				
		2D-6	A	M	R			C	R	R	R	C	R	R	R	R	R	R	R		R		R	R		R	R	R		R		R	R	R	R		R	
		2D-5	A	M	R	R	R	F		R	R	C	R	R	R	R			R				R	R		R	R		R	R	R	R	R	R				
		2D-4	A	M	R	R		C	R	R	R	C	R		R	R	R	R	R		R			?		F	R				R			R				
		2E-3	C	P/M		R		F	R		R	F	R	R	R			R	R					R		R	R	R	R	R	R	R		R		R		
		2E-2	C	P/M				F	R			F	R	R	R				R					R		R	R	R		R	?	?	R	R		R		
		2E-1	F	P/M		R		R	R			R	R	R											R		R	R	R	R	R	R		R				
		11H-1	R	P/M				R				R	R	R													R		R		R	R		R		R	R	
		11H-2	C	P/M		R		R	R		R	F	R	R												R	R	R				R	R	R	R	R		
		11H-3	F	P/M				R				R	R										?				R						R	R				
		11H-4	F	P/M				R				R	R	R													R					R	R					
		11H-5	B																																			

AGE	SECTION	SAMPLES (B14-)	ABUNDANCE	PRESERVATION	*Calcidiscus pataecus*	*Calcidiscus* sp. (< 5 µm)	*Coccolithus miopelagicus*	*Coccolithus pelagicus*	*Coccosphere indet.*	*Coronocyclus nitescens*	*Cyclicargolithus abisectus* (>11 µm)	*Cyclicargolithus floridanus*	*Discoaster deflandrei*	*Discoaster* sp.	*Helicosphaera carteri*	*Helicosphaera euphratis*	*Helicosphaera granulata*	*Helicosphaera obliqua*	*Helicosphaera* sp.	*Helicosphaera* sp. *cf. H. recta*	*Pontosphaera multipora*	*Pontosphaera* sp.	*Pyrocyclus* sp.	*Reticulofenestra bisecta* (< 10 µm)	*Reticulofenestra daviesii*	*Reticulofenestra dictyoda*	*Reticulofenestra lockeri*	*Reticulofenestra minuta*	*Reticulofenestra* (3-5 µm)	*Reticulofenestra* (5-7 µm)	*Sphenolithus conicus*	*Sphenolithus dissimilis*	*Sphenolithus moriformis*	*Sphenolithus* sp.	*Thoracosphaera heimii*	*Thoracosphaera* sp.	*Thriquetrorhabdulus carinatus*	*Chiasmolithus* sp. (reworked)
EARLIEST MIOCENE	SECTION B	26F	B																																		
		26E	F	P/M					R			R	R	R	R					R							R	R			R		R	R	R			
		26D	C	M					C	R		R	C	R	R	R	R	R	R	R			R	R	R	F	R	R	F	F	R	R	R	R	R	R		
		26C	C	P/M	R				F	R		R	C		R										R	R	R		R	R			R	R	R	R		
		26B	C	P/M	R				F	R		R	F	R	R		R			R					?	?	F	R		R	F			R	R	R	R		
		26A	B																																			

TEXT-FIGURE 5
Abundance, preservation, and distribution of calcareous nannofossil species from Yesera de Amara (section A) and Las Tres Piramides (section B). The occurrence of key species in both assemblages suggest the same age. Shade taxa are included in the discussion. Abundance: Abundant (A), Common (C), Few (F), Rare (R), Questionable presence of this species (?) and Barren (B). Preservation: Good (G), Moderate (M), and Poor (P).

Occurrence of Helicosphaera carteri

The presence of *Helicosphaera carteri* in our samples constrains the age to early Miocene at its oldest, and is evidence for establishing that the sediments are no older than Miocene. The occurrence of *Helicosphaera carteri* is an indication of Neogene age and its FO is recognized in the earliest Miocene Zone NN1 (Young 1998). Most of the *Helicosphaera carteri* specimens observed in our samples are a little overgrown and others exhibit dissolution (Text-Figure 6, C; Plate 2, Fig. 1-2). Our assemblage contains continuous rare to frequent occurrence of *Helicosphaera carteri* (Text-Figure 5).

Backman el al. (2012) suggested the use of the abundance cross-over between *Helicosphaera carteri* and *Helicosphaera euphratis* within the Zone CNM3 (lower part of NN2 and CN1c) as presented by Fornaciari and Rio (1996) for ODP Hole 926B (western tropical Atlantic Ocean). The rarity of *Helicosphaera euphratis* (text-figure 5 and Plate 2, Fig. 7-8, 9-10) relative to *Helicosphaera carteri* could indicate an even younger age assignment (Fornaciari and Rio 1996; Backman et al. 2012). Nevertheless, the preservation made recognition of the helicosphaeres difficult, so most are classified as *Helicosphaera* sp.

On the other hand, *Helicosphaera carteri* was not recorded in the early Miocene Zone NN1 in some sites. Martini (1990) documented the occurrence of *Helicosphaera carteri* from a poorly defined zone NN3 (Site 682) and Zone NN6 (Site 688). Martini also described a lower Miocene sequence characterized by abundant siliceous components at Site 682. Lower Miocene biozones were combined as NN1/NN2 due to some missing markers at Site 688. Bown and Dunkley Jones (2012) did not record the occurrence of *Helicosphaera carteri* from Sites U1332- U1334 (IODP Expedition 320).

Some authors extend the FO of *Helicosphaera carteri* to Oligocene (e.g. Vathi 1998, in Albania; Holcová 2005, Central Paratethys). De Kaenel and Villa (1998) discussed this occurrence and described a *Helicosphaera* aff. *carteri* in this time interval. These species are described as *Helicosphaera ethologa* Bown (2005) and "like *H. carteri* but older (NP23-24) - also slits in central area and wing less developed" in Nannotax. In the equatorial Pacific, there is a similar example: Mejia et al. (2007) and Mejía-Molina et al. (2010) reported *Helicosphaera carteri* from the late Oligocene (NP25) from onshore (Arroyo Alférez and Estratigráfico 4, Colombia).

Occurrence of Cyclicargolithus abisectus (> 11 µm)

The occurrence of *Cyclicargolithus abisectus* in our samples, associated with *Helicosphaera carteri*, suggest that our assemblage represent an early Miocene age. The last occurrence of *Cyclicargolithus abisectus* is reported within NN1 by Young (1998), but they can range up to middle Miocene, Zone NN5 (e.g. Martini 1990, Table 5; Backman et al. 2012). The occurrence of *Cyclicargolithus abisectus* is relatively continuous throughout the productive samples in the sections A and B (text-fig. 5). Examples of both good and poor preservation are presented in Plate 1 (Figs. 1 and 2).

Occurrence of Triquetrorhabdulus carinatus

The occurrence of *Triquetrorhabdulus carinatus* in our samples, associated with *Helicosphaera carteri* and *Cyclicargolithus abisectus*, suggest that our assemblage represents an early Miocene age. Few specimens of *Triquetrorhabdulus carinatus* were observed in the upper part of the section A and in section B. Two examples are shown in Plate 2 (Fig. 24 and 25). Considering the preservation of the samples, most of the nannoliths could have been removed by diagenesis.

In the eastern equatorial Pacific, *Triquetrorhabdulus carinatus* is clearly recorded from late Oligocene to early Miocene. Martini (1990) documents the range of the *T. carinatus* from latest Oligocene (NP24/25) to early Miocene (NN2) at Leg 112 Site 682A. Bown and Dunkley Jones (2012) report the occurrence of *T. carinatus* from NP24 to NN2 (e.g. Sites U 1333A, Chart 3, p. 17, and U1334A, Chart 4, p.23). Agnini et al. (2014) reported the LO of *T. carinatus* in NN2. Onshore, Mejía-Molina et al. (2010) also documented *T. carinatus* from NP23 to NN2 in Colombia.

Occurrence of Sphenoliths

Based on the extent of recrystallization of most of the nannofossils and especially sphenoliths, we do not consider them diagnostic to the assemblage. Most of the sphenoliths were difficult (or impossible) to identify to the species level and are classified as *Sphenolithus* sp. The samples from both Sections A and B contain rare *Sphenolithus conicus* (Plate 2, Fig. 16-19), *Sphenolithus dissimilis* (Plate 2, Fig. 22-23), and *Sphenolithus moriformis* (Plate 2, Fig. 20-21).

The absence of *Sphenolithus ciperoensis* and *Sphenolithus delphix* in the samples suggests the assemblage is not older than Miocene, although their absence might be related to preservation or ecology. A similar problem of poorly preserved or missing sphenolithus is observed in Leg 112 for the upper Oligocene. The rare occurrence of *Sphenolithus* in the assemblage might be related to their preference for warmer temperatures (Bralower 2002; Tremolada and Bralower 2004; Kalb and Bralower 2012). The location of this study is related to cold upwelling water that could influence the distribution and abundance of taxa in this area (Lyle et al. 2008). However, we conclude that the absence of *Sphenolithus ciperoensis* and *Sphenolithus delphix* indicates a Miocene age. *Sphenolithus ciperoensis* and *Sphenolithus delphix* are reported in the equatorial Pacific (e.g. Bown and Dunkley Jones 2012; Agnini et al. 2014).

Implications for Pisco-Chilcatay boundary

As sequence stratigraphic models for the Pisco Basin develop, there is clearly a need for improved chronostratigraphic calibration of lithostratigraphic units in the basin, including for the Chilcatay and base of the Pisco Formations. This study provides biostratigraphic data which will help to build consensus on events in the upper part of the Chilcatay Formation and the boundary between the Chilcatay and Pisco formations that augment other reports (e.g. León et al. 2008; DeVries and Jud 2018; Di Celma et al. 2018). Di Celma et al.'s (2018) geologic map and stratigraphic description place all of our sections A and B within the Chilcatay Formation. They report a date from a tuff of 17.99 Ma, from 1 m below the top of the Chilcatay Formation and two occurrences of *Discoaster druggi* and *Sphenolithus belemnos* at Yesera de Amara. Since they did not provide coordinate locations for the collected samples at Yesera de Amara, we are not able to correlate those results precisely with our sections. They provide a range chart but did not include any photomicrographs of representative species supporting their

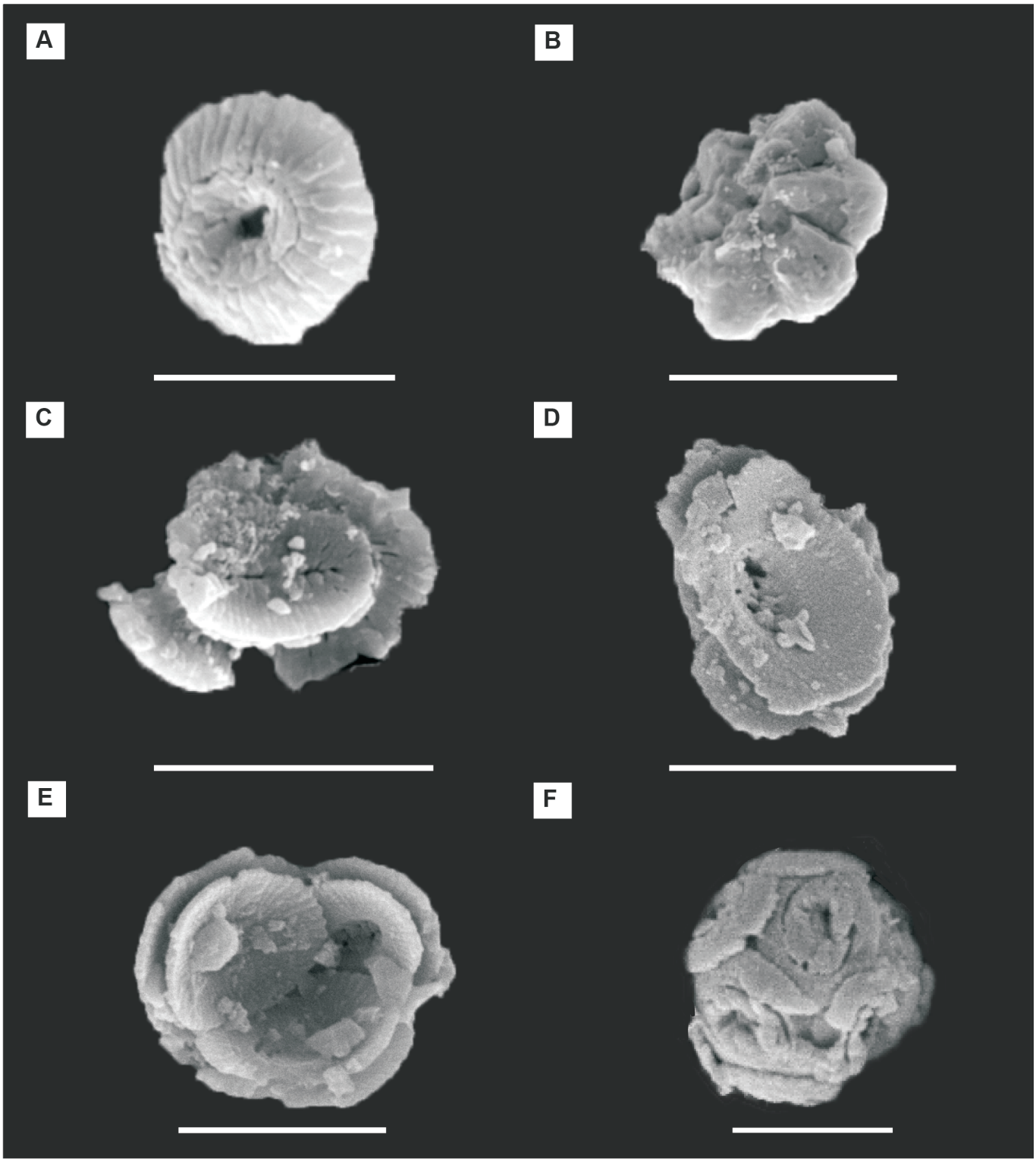

TEXT-FIGURE 6
Scanning electron microscope (SEM) photographs showing range of preservation with selective dissolution and overgrowth. (A) *Coccolithus pelagicus*, distal view, with minor overgrowth on specific elements on distal shield. (B) *Discoaster* sp., overgrowth formation is around the central area and along the rays. (C) *Helicosphaera carteri*, proximal view, exhibits dissolution on the outer cycle and some overgrowth. (D) *Reticulofenestra* sp., shows dissolution on the central area and proximal shield. (E) Coccosphere of *Reticulofenestra* sp., proximal view. (F) Coccosphere of *Cyclicargolithus floridanus*, distal view. A, B, C, and E from sample B14-3B-14; D and F from sample B14-3B-15. All scale bars = 5μm.

conclusions. Our assemblage contains poorly preserved discoasterids and we were not able to definitively identify *Discoaster druggi*.

CONCLUSIONS

The present study documents a biostratigraphic analysis of calcareous nannofossils from sediments collected from Yesera de Amara and Las Tres Piramides in the Pisco Basin. These results from nannofossil biostratigraphy contribute to the local stratigraphy in the basin and to regional biostratigraphy of the earliest Miocene. This research is one of the few reports of calcareous nannofossil from the early Miocene of the low latitude eastern Pacific.

Correlation of outcrops following two lithostratigraphic markers across the study area helped to identify the sections for this study. Of the six sections measured, only two demonstrated optimal preservation and were considered for biostratigraphic conclusions. Analysis of the species distribution in section A (Yesera de Amara) and section B (Las Tres Piramides) suggests the same age for the assemblages. Abundance and preservation of species ranges from rare to common and poor to moderate, respectively. However, the overall abundance and preservation considerably decrease in section B, and might be related to their coarser grain size than in section A.

Due to most of the discoasters and sphenoliths showing strong recrystallization and dissolution, we are using *Helicosphaera carteri* to constrain the age of the sections to early Miocene. *Helicosphaera carteri* in association with *Cyclicargolithus abisectus*, *Reticulofenestra bisecta*, and *Triquetrorhabdulus carinatus*, suggest that the assemblage recovered from sections A and B represent an age of earliest Miocene (Zone NN1/CN1b). The rarity of *Helicosphaera euphratis* relative to *Helicosphaera carteri* could indicate an even younger age assignment, although poor preservation precludes a reliable assessment of helicosphere relative abundances. Although *Cyclicargolithus abisectus* can range up to NN5 and *Triquetrorhabdulus carinatus* up to NN2, the absence of *Discoaster druggii* might suggest that the assemblage is not younger than NN1. The absence of *Sphenolithus ciperoensis* and *Sphenolithus delphix* in the samples suggest the assemblage is not older than Miocene.

In general, studies from the equatorial Pacific region indicate some difficulties in the description of the earliest Miocene, Zone NN1. This could be due to the low occurrence or absence of the species markers, or confusion with species identification. For example, *Reticulofenestra bisecta* becomes rare and discontinuous in late Oligocene and into the NN1 and *Helicosphaera carteri* is sometimes misidentified with *Helicosphaera ethologa*.

ACKNOWLEDGMENTS

This study was supported by the Geoscience Research Institute and Department of Earth and Biological Sciences, Loma Linda University. We would like to acknowledge Andrea Concheyro from University of Buenos Aires (Argentina) for helping us with the identification of calcareous nannofossils. We especially thank the editor Jean Self-Trail and reviewers Denise Kulhanek and Cherry Newsam for their important suggestions and contributions to improve this paper. We thank Kenneth Finger from the Museum of Paleontology- University of California Berkeley and Angelo Plata from Universidad de Salamanca (Colombia) for helping with foraminifera and diatoms, respectively. We thank Mario Urbina from the Museo de Historia Natural (Peru) for help with field locations and Orlando Poma from Universidad Peruana Union (Peru) for assistance with mapping in the field. We also thank Robert Adorno and Lily Hufmann for helping with sample collection.

REFERENCES

AGNINI, C., FORNACIARI, E, RAFFI, I., CATANZARITI, R., PÄLIKE, H., BACKMAN, J. and RIO, D., 2014. Biozonation and biochronology of Paleogene calcareous nannofossils from low and middle latitudes. *Newsletters on Stratigraphy*, 47: 131–181.

BACKMAN, J., RAFFI, I., RIO, D., FORNACIARI, E. and PÄLIKE, H., 2012. Biozonation and biochronology of Miocene through Pleistocene calcareous nannofossils from low and middle latitudes. *Newsletters on Stratigraphy*, 45: 221–244.

BELIA, E. R., NICK, K. E., BEDOYA AGUDELO, E. and CONCHEYRO, A., 2015. "Late Oligocene – early Miocene Calcareous Nannofossils from basal Pisco Formation, Pisco Basin, Peru." *Journal of Nannoplankton Research*, INA abstracts, Bohol, Philippines, 35: 22.

BELIA, E. R. and NICK, K. E., 2016. "Early-Miocene Calcareous Nannofossil Biostratigraphy from the low-latitude, Pisco Basin, Peru". Geological Society of America *Abstracts with Programs*, 48: 4.

BLAJ, T., BACKMAN J. and RAFFI I., 2009. Late Eocene to Oligocene preservation history and biochronology of calcareous nannofossils from Paleo-Equatorial Pacific Ocean sediments. *Rivista Italiana di Paleontologia e Stratigrafia*, 115: 67–85.

BOWN, P. R. and DUNKLEY JONES, T., 2012. Calcareous nannofossils from the Paleogene equatorial Pacific (IODP 320 Sites U1331–1334). *Journal of Nannoplankton Research,* 32: 3–51.

BOWN, P. R. and YOUNG, J. R., 1998. Techniques. In: Bown, P. R., Ed., *Calcareous Nannofossil Biostratigraphy*. British Micropaleontological Society Publication Series. London: Chapman & Hall, 16–28.

BUKRY, D., 1973. Low-latitude coccolith biostratigraphic zonation, *Initial Report Deep Sea Drill*. Project 15: 685–703.

BRALOWER, T. J., 2002. Evidence of surface water oligotrophy during the Paleocene-Eocene thermal maximum: Nannofossil assemblage data from Ocean Drilling Program Site 690, Maud Rise, Weddell Sea. *Paleoceanography*, 17: 1–9.

DE KAENEL, E. and VILLA, G.,, 1996. Oligocene-Miocene calcareous nannofossil biostratigraphy and paleoeecology from the Iberian Abyssal Plain. *Proceedings of the Ocean Drilling Program. Scientific Results*, 149: 79–145.

———, 1998. *Helicosphaera carteri*: a further note on its stratigraphical occurrence. *Journal of Nannoplankton Research*, 20 (2): 105–106.

DEVRIES, T. J., 1988. Paleoenvironments of the Pisco Basin. In: R. B. Dunbar and P. A. Baker, Eds., *Cenozoic Geology of the Pisco Basin*, IGCP no.156 Guidebook to Field Workshop, May 1988, Lima, pp. 41 50.

DEVRIES, T. J., 1998. Oligocene deposition and Cenozoic sequence boundaries in the Pisco Basin (Peru). *Journal of South American Earth Sciences*, 11: 217–231.

DEVRIES, T.J. and JUD, N. A., 2018. Lithofacies patterns and paleogeography of the Miocene Chilcatay and lower Pisco

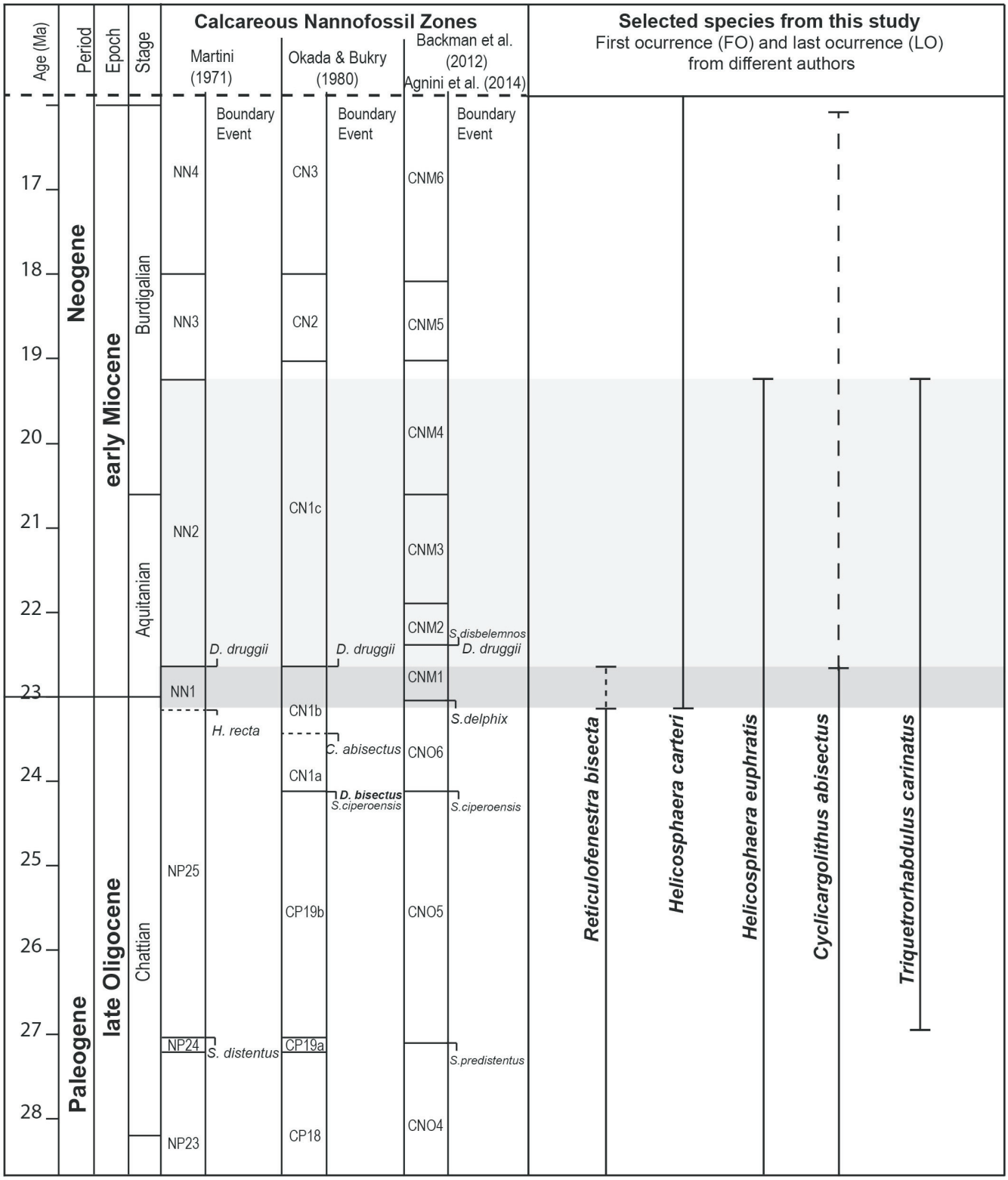

TEXT-FIGURE 7
Stratigraphic subdivisions, standard zonations of calcareous nannofossils (modified from Backman et al. 2012 and Agnini et al. 2014), and selected species from this study. The occurrence of *Helicosphaera carteri* associated with *Reticulofenestra bisecta* (<10 μm), *Cyclicargolithus abisectus* and *Triquetrorhabdulus carinatus* suggest an age of earliest Miocene, Zone NN1 (CN1b). All other taxa present in the assemblage are consistent with this assignment.

depositional sequences (East Pisco Basin, Peru). *Boletin de la Sociedad Geológica del Perú*, 8: 124–167.

DEVRIES, T. J., NAVAREZ, Y., SANFILIPPO, A., MALUMIAN, N. and TAPIA P., 2006. New microfossil evidence for a late Eocene age of the Otuma Formation (Southern Peru). XIII Congreso Peruano de Geología, Lima, Peru. October: 615–618.

DEFLANDRE, G., 1952. Classe des Coccolithophoridés. (Coccolithophoridae. Lohmann, 1902). In: Grassé, P. P., Ed., *Traite de Zoologie***.** Paris: Masson, pp. 439–470.

DEFLANDRE, G. and FERT, C., 1954. Observations sur les coccolithophoridés actuels et fossiles en microscopie ordinaire et électronique. *Annales de Paléontologie*, 40: 115–176.

DI CELMA, C., MALINVERNO, E., BOSIO, G., COLLARETA, A., GARIBOLDI, K., GIONCADA, A. and BIANUCCI, G., 2017. Sequence stratigraphy and paleontology of the upper Miocene Pisco Formation along the western side of the lower Ica valley (Ica Desert, Peru). *Rivista Italiana di Paleontologia e Stratigrafia* (Research in Paleontology and Stratigraphy), 123, 255–274.

DUNBAR, R. B., MARTY, R. C. and BAKER, P. A., 1990. Cenozoic marine sedimentation in the Sechura and Pisco basins, Peru. *Palaeogeography, Palaeoclimatology, Palaeoecology*, 77: 235–261.

FOURTANIER, E. and MACHARÉ, J., 1988. Late Eocene to Pliocene marine diatoms from Peru. In: F. E. Round, Ed., Proceedings of the 9th International Diatom Symposium, (Bristol, August 24–30, 1986.) Koenigstein, Germany: Biopress Ltd. and Koeltz Scientific Books, 15: 1–163.

FORNACIARI, E. and RIO, D., 1996. Latest Oligocene to early middle Miocene quatitative calcareous nannofossil biostratigraphy in the Mediterranean region. *Micropaleontology*, 42:1–36.

GRADSTEIN, F. M., OGG, J. G., SCHMITZ, M. D. and OGG, G. M., 2012. *The Geologic Time Scale 2012*. Amsterdam: Elsevier, 876–877.

HAY, W. W., MOHLER, H. P., ROTH, P. H., SCHMIDT, R.R. and BOUDREAUX, J.E., 1967. Calcareous nannoplankton zonation of the Cenozoic of the Gulf Coast and Caribbean-Antillean area, and transoceanic correlation. *Transactions of the Gulf Coast Association of Geological Societies*, 17: 428–480.

HOLCOVÁ, K., 2005. Quantitative calcareous nannoplankton biostratigraphy of the Oligocene/Miocene boundary interval in the northern part of the Buda Basin (Central Paratethys). *Geological Quarterly*, 49: 263–274.

KALB, A. L. and BRALOWER, T., 2012. Nannoplankton origination events and environmental changes in the late Paleocene and early Eocene. *Marine Micropaleontology*, 92–93, 1–15.

KALLANXHI, M. E., ĆORIĆ, S. and KOÇIU, A., 2016. Late Oligocene calcareous nannofossils from Albanian-Thessalian Intramontane Basin (Bozdovec Section, Albania)–a quantitative approach. *Studia UBB Geologia*, 60: 5–20.

PLATE 1

Photomicrographs of calcareous nannoplankton from Cerro Yesera de Amara (section A) and Las Tres Piramides (section B), Pisco Basin. All photographs taken with crossed polarizers unless otherwise noted.

1–2 *Cyclicargolithus abisectus* (> 11 µm), (1) sample B14-2D-4, (2) sample B14-3C-11

3 C*yclicargolithus floridanus,* sample B14-3A-19

4–5 *Coccolithus miopelagicus* (>13 µm), (5) phase contrast, sample B14-3B-15

6–7 *Coccolithus pelagicus,* (7) phase contrast, sample B14 2D-4

8–9 *Reticulofenestra dictyoda,* (9) phase contrast, sample B14-2D-5

10–11 *Reticulofenestra daviesii,* sample B14-3B-15, (11) same specimen rotated

12–13 *Reticulofenestra lockeri*, sample B14-3B-14, (13) same specimen rotated

14–15 *Reticulofenestra bisecta* (10 µm), sample B14-2D-5, (15) same specimen rotated

16–17 *Reticulofenestra bisecta* (7 µm), sample B14-2D-5, (17) same specimen rotated

18 *Reticulofenestra* sp. (5–7µm), sample B14-3B-15

19 *Reticulofenestra* sp. (3–5 µm), sample B14-3B-14

20 *Reticulofenestra minuta,* sample B14-3A-19

21 *Pyrocyclus* sp., sample B14-3B-15

22 *Coronocyclus nitescens,* sample B14-3A-19

23–24 *Chiasmolithus* sp., (24) phase contrast, sample B14-3A-19

25–26 *Pontosphaera* sp., (26) same specimen rotated, sample B14- 3A-17

27–28 *Pontosphaera multiporata,* (28) same specimen rotated, sample B14-3A-17

29 *Calcidiscus pataecus,* phase contrast, sample B14-2D-5

30 *Calcidiscus pataecus,* phase contrast, sample B14-3B-14

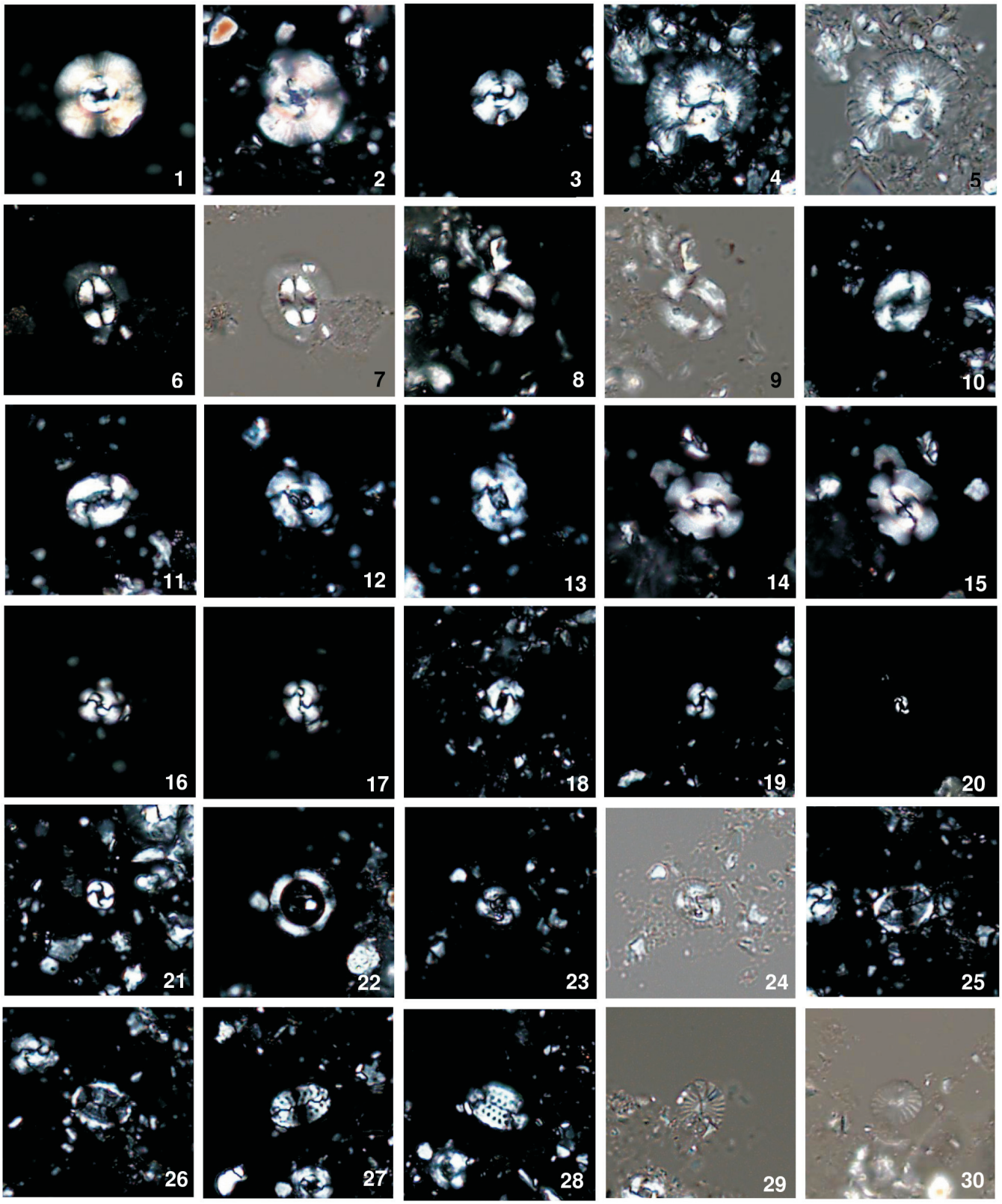
1
2
3
4
5
6
7
8
9
10
11
12
13
14
15
16
17
18
19
20
21
22
23
24
25
26
27
28
29
30

KAMIKURI, S. and MOORE T. C., 2017. Reconstruction of oceanic circulation patterns in the tropical Pacific across the early/middle Miocene boundary as inferred from radiolarian assemblages. *Palaeogeography*, *Palaeoclimatology*, *Palaeoecology*, 487: 136–148.

KENNETT, J. P., KELLER, G. and SRINIVASAN, M. S., 1985. Miocene planktonic foraminiferal biogeography and paleogeographic development of the Indo-Pacific region. *Geological Society of America Memoir* 163. 197–236.

KLEIN, G. D., ZÚÑIGA Y RIVERO, F.J., HAY-ROE, H. and ALVAREZ-CALDERON, E., 2011. A Reappraisal of the Mesozoic/Cenozoic Tectonics and Sedimentary Basins of Peru. AAPG Search and Discovery Article #10332.

LEÓN, W., ALEMAN, A., ROSELL, W., TORRRES, V. and DE LA CRUZ, O., 2008. Estratigrafia, sedimentologia y evolucion tectonica de la cuenca Pisco Oriental, Peru. Volumen Estudios Regionales, INGEMMET. Lima, Perú. Boletín 27

LOPEZ RAMOS, E., 2009. *Évolution tectono-stratigraphique du double bassin avant-arc de la marge convergente Sud Colombienne-Nord Équatorienne pendant le Cénozoïque* (Doctoral dissertation), University of Nice Sophia Antipolis, Nice, France.

LYLE, M., BARRON, J., BRALOWER, T. J., HUBER, M., OLIVAREZ LYLE, A., RAVELO, A. C., REA, D. K. and WILSON P. A., 2008. Pacific Ocean and Cenozoic evolution of climate. *Reviews of Geophysics*, 46: 1–47.

MAIORANO, P. and MONECHI, S., 2006. Early to late Oligocene calcareous nannofossils bioevents in the Mediterranean (Umbria-Marche Basin, Central Italy). *Rivista Italiana di Paleontologia e Stratigrafia* (Research In Peleontology and Stratigraphy), [S.I.], 112 (2).

MARTINI, E., 1971. Standard tertiary and Quaternary calcareous nannoplankton zonation. In: Farinacci, A. (Ed.), *Proceedings II Planktonic Conference, Rome, 1970*. Telao Scienza, Rome, 2: 739–785.

———, 1990. Tertiary and Quaternary calcareous nannoplankton biostratigraphy off Peru (ODP LEG 112): Proceedings of the Ocean Drilling Program, Scientific Results, v. 112.

MARTY, R., DUNBAR, R., MARTIN, J. B. and BAKER, P., 1988. Late Eocene diatomite from the Peruvian coastal desert, coastal upwelling in the eastern Pacific, and Pacific circulation before the terminal Eocene event. *Geology*, 16: 818–822.

MEJÍA, A. E., FLORES, J. A. and TORRES, V., 2007. Nanofósiles calcáreos de la sección Arroyo Alférez (Carmen de Bolívar): una biozonificación preliminar para el oligoceno–mioceno medio del norte de colombia. *Boletín de Geología*, 29: 21–28.

MEJÍA-MOLINA, A. M., 2010. "*Biostratigrafía y Biocronología de Nannofósiles Calcareous de Mioceno en el Norte de Colombia y Caribe*" Ph. D. dissertation, Universidad de Salamanca. https://gredos.usal.es/jspui/.../DGL%20_MejíaMolina_Alejandra_Bioestratigrafía.pdf

MEJÍA-MOLINA, A. M., FLORES, J. A., TORRES-TORRES, V. and SIERRO, F. J., 2010. Distribution of Calcareous nannofossils in Upper Eocene-Upper Miocene deposits from Northern Colombia and the Caribean Sea. *Revista española de micropaleontologia*, 42: 279–300.

PLATE 2

Cont. Photomicrographs of calcareous nannoplankton from Cerro Yesera de Amara (section A) and Cerro Las Tres Piramides (section B), Pisco Basin.
All photographs taken with crossed polarizers unless otherwise noted.

1–2 *Helicosphaera carteri*, (2) same specimen rotated, sample B14-2D-5

3–4 *Helicosphaera granulata*, (4) same specimen rotated, sample B14-2D-4

5–6 *Helicosphaera obliqua*, (6) same specimen rotated, sample B14-3A-19

7–8 *Helicosphaera euphratis*, (8) same specimen rotated, sample B14-3A-17

9–10 *Helicosphaera euphratis*, (10) same specimen rotated, sample B14-2D-5

11–12 *Helicosphaera* sp. *cf. H. recta*, (12) same specimen rotated, sample B14-3A-19

13 *Discoaster* sp., phase contrast, sample B14-3A-17

14 *Discoaster* sp., phase contrast, sample B14-2E-3

15 *Discoaster deflandrei*, phase contrast, sample B14-2D-5

16–19 *Sphenolithus conicus*, (16–17) sample B14-3A-17, (17) same specimen rotated; (18–19) sample B14-3C-11, (19) same specimen rotated

20–21 *Sphenolithus moriformis*, sample B14-3B-16, (21) same specimen rotated

22–23 *Sphenolithus dissimilis*, (23) same specimen rotated, sample B14-2D-5

24–25 *Triquetrorhabdulus carinatus*, (24) B14-3A-18, (25) sample B14-26D-5

26 *Thoracosphaera heimii*, sample B14-3A-18

27–30 *Coccosphere indet*., (27–28) sample B14-3A-19, (29-30) sample B14-2D-4

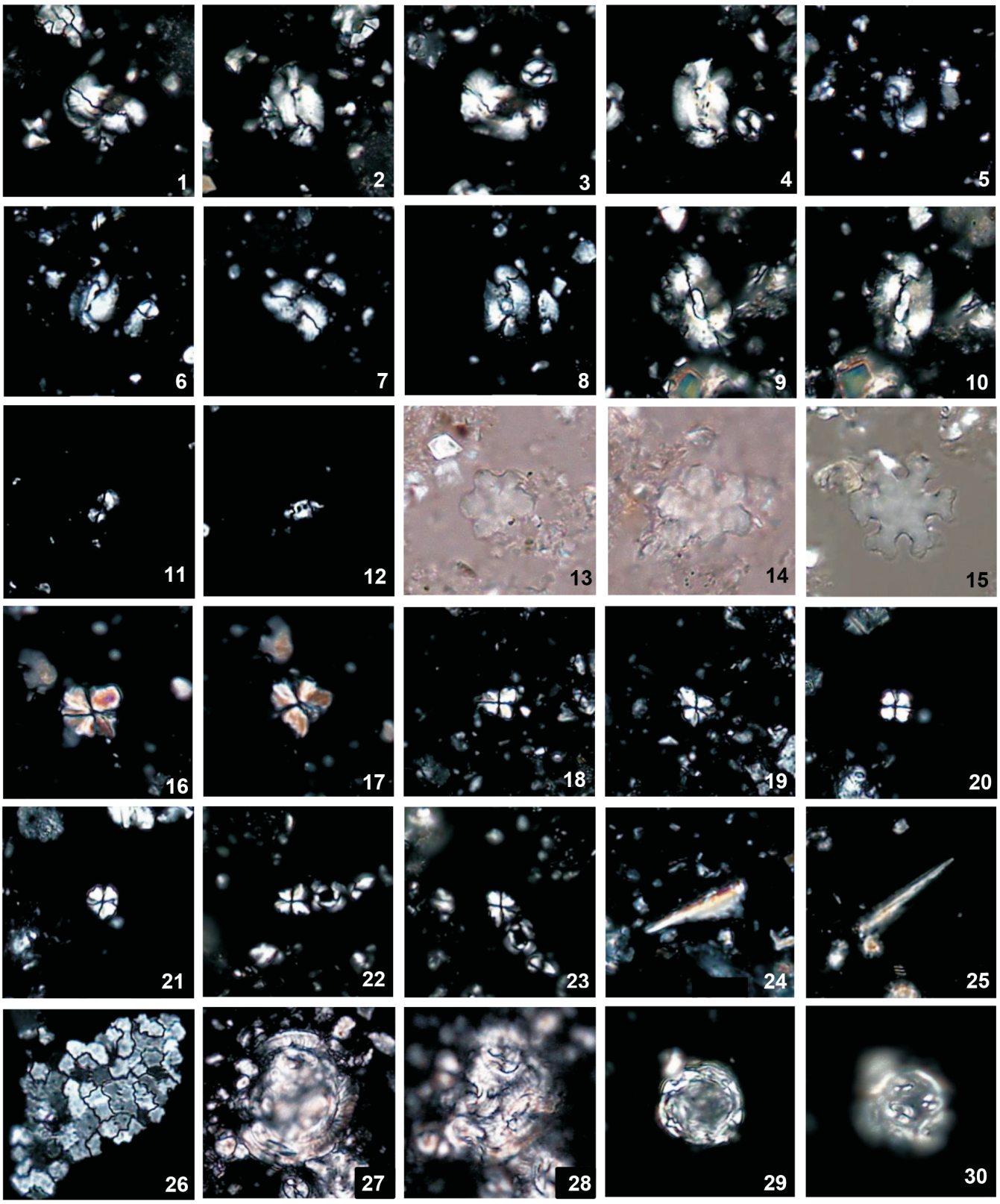
1
2
3
4
5
6
7
8
9
10
11
12
13
14
15
16
17
18
19
20
21
22
23
24
25
26
27
28
29
30

OKADA, H. and BUKRY, D., 1980. Supplementary modification and introduction of code numbers of the low-latitude coccolith biostratigraphic zonation (Bukry 1973, 1975). *Marine Micropaleontology* 5: 321–325.

PÄLIKE, H., NISHI, H., LYLE, M., RAFFI, I., GAMAGE, K., KLAUS, A. and THE EXPEDITION 320/321 SCIENTISTS, 2010. Expedition 320/321 summary. In: Pälike, H., Lyle, M., Nishi, H., Raffi, et al., *Pacific equatorial transect,* 1–141. Tokyo: Integrated Ocean Drilling Program Management International, Inc. IODP Proceedings, 320/321.

PERCH-NIELSEN, K., 1979. Calcareous nannofossil zonation at the Cretaceous/Tertiary boundary in Denmark. In: Birkelund, T. and Bromley, R. G., Eds., *Proceedings, Cretaceous-Tertiary Boundary Events Symposium,* Copenhagen, 1:115–135.

———, 1985. Cenozoic Calcareous nannofossils. In: Bolli, H. M., Saunders, J. B., and Perch-Nielsen, K., Eds.. *Plankton Stratigraphy*, CAmbridge: Cambridge University Press, 427–554.

RAFFI, I., BACKMAN, J., FORNACIARI, E., PÄLIKE, H., RIO, D., LOURENS, L. and HILGEN, F., 2006. A review of calcareous nannofossil astrobiochronology encompassing the past 25 million years. *Quaternary Science Reviews*, 25: 3113–3137.

ROTH, P. H. and THIERSTEIN, H., 1972. Calcareous nannoplankton: Leg 14 of the Deep Sea Drilling Project. In: Hayes, D. E. and Pimm A. C., Eds., *Initial Reports of the Deep Sea Drilling Project*. Washington. D.C.: U.S. Government Printing Office, 14: 421–485.

SIESSER, W. G., WARD, D. J. and LORD, A. R., 1987. Calcareous nannoplankton biozonation of the Thanetian Stage (Paleocene) in the type area. *Journal of Micropaleontology*, 6: 85–102.

STRADNER, H. and EDWARDS, A. R., 1968. Electron microscopic studies on Upper Eocene coccoliths from the Oamaru Diatomite, New Zealand. *Jahrbuch der Geologischen Bundesanstalt*, 13 (66): 1–48.

SUESS, E., VON HUENE, R. et al., 1988. *Proceeding ODP, Initial Repots.,* 112. College Station, TX: Ocean Drilling Program.

THORNBURG, T. and KULM, L. D., 1981. Sedimentary basins of the Peru continental margin: Structure, stratigraphy and Cenozoic tectonics from 6 ° to 16°S latitude. In: L. D. Kulm, J. Dymond, E. J. Dasch and D. M. Hussong, Eds., Nazca Plate: Crustal Formation and Andean Convergence. *Geological Society of America Memoir* 154: 393–422.

TREMOLADA, F. and BRALOWER, T. J., 2004. Nannofossils Assemblage Fluctuations during the Paleocene-Eocene Thermal Maximum at Site 213 (Indian Ocean) and 401 (North Atlantic Ocean): Paleoceanographic Implications. *Marine Micropaleontology*, 52, 107–116.

VAROL, O., 1989. Paleogene calcareous nannofossil biostratigraphy. In: Crux, J.A. and van Heck, S. E., Eds., *Nannofossils and their applications.* British Micropaleontological Society series, 267–310.

VATHI, K., 1998. A note on the first occurrence of *Helicosphaera carteri* in the Early Oligocene (NP23, *Sphenolithus predistentus* Zone). *Journal of Nannoplankton Research*, 20 (1): 39–43.

WEI, W. and WISE, S. W. JR., 1990. Biogeographic gradients of middle Eocene-Oligocene calcareous nannoplankton in the South Atlantic Ocean. *Palaeogeography*, *Palaeoclimatology*, *Palaeoecology*, 79: 29–61.

WEI, W., VILLA, G. and WISE, S. W., 1992. Paleoceanographic implications of Eocene–Oligocene calcareous nannofossils from Sites 711 and 748 in the Indian Ocean. In: Wise Jr., S. W., Schlich, R. et al., *Proceedings of the Ocean Drilling Program, Scientific Results,* College Station, TX, 120: 979–999.

YOUNG, J. R., 1998. Neogene. In: Bown, P. R., Ed., *Calcareous Nannofossil Biostratigraphy*. British Micropaleontological Society Publications Series. London: Chapman & Hall, 225–265.

APPENDIX 1

Coordinates, number of samples collected, and nannofossil data from the additional sections. A total of 20 samples were collected and analyzed. The general abundance is few to rare and the preservation is poor in all the productive samples.

Location ID	Latitude	Longitude	# Collected samples	# Productive samples
Section A-2 (Cerro Yesera de Amara)	-14.58651944	-75.68049722	5	2
Section C (Yesera de Amara, lower part)	-14.59288333	-75.67092778	5	2
Section C (Yesera de Amara, upper part)	-14.59398333	-75.67291389	3	3
Section D (Submarino area)	-14.59941944	-75.66347778	5	1
Section E (Sumbarino area)	-14.59998889	-75.65314722	2	2
Total			20	10

APPENDIX 2

Alphabetical list of calcareous nannofossil species cited in the text and figures:

Calcidiscus Kamptner 1950

Calcidiscus pataecus (Gartner 1967) de Kaenel and Villa 1996

Chiasmolithus Hay et al. 1966

Coccolithus miopelagicus Bukry 1971

Coccolithus pelagicus (Wallich 1877) Schiller 1930

Coronocyclus nitescens (Kamptner 1963) Bramlette and Wilcoxon 1967

Cyclicargolithus abisectus (Muller 1970) Wise 1973

Cyclicargolithus floridanus (Roth and Hay, *in* Hay et al. 1967) Bukry 1971

Discoaster Tan 1927

Discoaster deflandrei Bramlette and Riedel 1954

Helicosphaera Kamptner 1954

Helicosphaera carteri (Wallich 1877) Kamptner 1954

Helicosphaera euphratis Haq 1966

Helicosphaera granulata (Bukry and Percival 1971) Jafar and Martini 1975

Helicosphaera obliqua Bramlette and Wilcoxon 1967

Helicosphaera recta (Haq 1966) Jafar and Martini 1975

Pontosphaera Lohmann 1902

Pontosphaera multipora (Kamptner 1948 ex Deflandre *in* Deflandre and Fert 1954) Roth 1970

Pyrocyclus Hay and Towe 1962

Reticulofenestra Hay, Mohler and Wade 1966

Reticulofenestra bisecta (Hay, Mohler and Wade 1966) Roth 1970

Reticulofenestra daviesii (Haq 1968) Haq 1971

Reticulofenestra dictyoda (Deflandre *in* Deflandre and Fert 1954) Stradner *in* Stradner and Edwards 1968

Reticulofenestra lockeri Müller 1970

Reticulofenestra minuta Roth 1970

Sphenolithus Deflandre *in* Grassé 1952

Sphenolithus conicus Bukry 1971

Sphenolithus dissimilis Bukry and Percival 1971

Sphenolithus moriformis (Brönnimann and Stradner 1960) Bramlette and Wilcoxon 1967

Thoracosphaera Kamptner 1927 (*sensu lato*)

Thoracosphaera heimii (Lohmann 1920) Kamptner 1944

Triquetrorhabdulus carinatus Martini 1965